71794-CR

42 P.

A TRANSPORT MODEL OF THE TURBULENT SCALAR-VELOCITY

May 1987

R. S. Amano
Principal Investigator

and

P. Goel and J. C. Chai
Research Assistants

Department of Mechanical Engineering
University of Wisconsin--Milwaukee
Milwaukee, Wisconsin 53201
U.S.A.

Status Report

(NASA-CR-180605) A TRANSPORT MODEL OF THE TURBULENT SCALAR-VELOCITY Status Report, Feb. - May 1987 (Wisconsin Univ.) 42 p
Avail: NTIS HC A03/MF A01 CSCL 20D

N87-22160

Unclas
G3/34 0071794

The report documents research completed during the period of February 1987 through May 1987 under NASA-Marshall Space Flight Center Research Grant No. NAG 8-617.

332E/3389E

ABSTRACT

This study represents performance tests of the third-order turbulence closure for predictions of separating and recirculating flows in backward-facing step. Computations of the momentum and temperature fields in the flow domain being considered entail the solution of the time-averaged transport equations containing the second-order turbulent fluctuating products. The triple products, which are responsible for the diffusive transport of the second-order products, attain greater significance in separating and reattaching flows. Formulations have been made for those products mentioned above by developing each corresponding transport equation. A low Reynolds number model associated with the viscous effect in near-wall regions is developed and incorporated.

The computations are compared with several algebraic models and with the experimental data. The predication has been improved considerably, particularly in the separated shear layer.

Computations are further made for the temperature-velocity double products and triple products. Although there is not any appropriate experimental data to compare, the present computations are compared to the results obtained by solving the several existing algebraic correlations. The agreement between these sets is shown to be quite reasonable.

Finally, several advantages have been observed in the usage of the transport equations for the evaluation of the turbulence triple products; one of the most important features is that the transport model can always take the effects of convection and diffusion into account in strong convective shear flows such as reattaching separated layers while conventional algebraic models cannot account for these effects in the evaluation of turbulence variables.

NOMENCLATURE

C_f	wall skin friction coefficient, $\tau_w/(1/2)\rho U_{IN}^2$
C_g	constant used in turbulence model
$C_{i\theta,1}, C_{i\theta,2}$	coefficients for the pressure-heat flux term in the transport equation of $\langle u_i\theta \rangle$
C_{1T}, C_{2T}	coefficients in the algebraic expressions for $\langle u_i\theta \rangle$
$C_\gamma, C_{\gamma w}$	coefficients for the pressure-stress and the near-wall low-Reynolds number model of the transport equations of $\langle u_i u_j u_k \rangle$
$C_{\epsilon\gamma}$	coefficient for the dissipation rate in the transport equations of $\langle u_i u_j u_k \rangle$
C_μ	coefficient for the determination of turbulent viscosity ($\simeq 0.09$)
$C_{\theta\gamma}$	coefficient for the pressure-heat flux term in the transport equation of $\langle u_i u_j \theta \rangle$
$C_{\theta\epsilon}$	coefficient for the dissipation rate in the transport equation of $\langle u_i u_j \theta \rangle$
c_p	specific heat of fluid
C_p	wall static pressure coefficient, $(P_w - P_{IN})/(1/2)\rho U_{IN}^2$
D_c	depth of the channel ($Y_o + H$)
D_{ij}	diffusion rate of Reynolds stresses, $\langle u_i u_j \rangle$
D_{ijk}	diffusion rate of triple-velocity products, $\langle u_i u_j u_k \rangle$
$D_{i\theta}$	diffusion rate of the heat flux, $\langle u_i\theta \rangle$
$D_{ij\theta}$	diffusion rate of the triple products of velocity and temperature, $\langle u_i u_j \theta \rangle$
H	step height

k	turbulent kinetic energy
p	pressure fluctuation
P	mean pressure
P_{ij}	production rate of Reynolds stresses, $\langle u_i u_j \rangle$
$P_{ijk,1}$	production rate of triple velocity products, $\langle u_i u_j u_k \rangle$, due to mean strain rates
$P_{ijk,2}$	production rate of triple velocity products, $\langle u_i u_j u_k \rangle$, due to interaction of the Reynolds stresses with their gradients
$P_{i\theta}$	production rate of $\langle u_i \theta \rangle$
$P_{ij\theta,1}$	production rate of $\langle u_i u_j \theta \rangle$ due to mean strain rates and temperature gradients
$P_{ij\theta,2}$	production rate of $\langle u_i u_j \theta \rangle$ due to Reynolds stresses and the heat fluxes interacting with their gradients
Pr	molecular Prandtl number
Pr_t	turbulent Prandtl number
q_w	wall heat flux per unit area
T	mean temperature
T_{IN}	inlet stream temperature
u	fluctuating velocity in x-direction
U	mean velocity in x-direction
U_{IN}	inlet stream velocity
v	fluctuating velocity in y-direction
V	mean velocity in y-direction
x_r	reattaching point
x'	normalized coordinate = $(x - x_r)/x_r$
x, y	Cartesian coordinates
x_n	normal distance from the wall
Y_o	height of the channel upstream of the step

Greek Symbols

α	thermal diffusivity
δ_{ij}	Kronecker delta
ε	dissipation rate of turbulent kinetic energy
ε_{ij}	dissipation rate of Reynolds stresses, $\langle u_i u_j u_k \rangle$
ε_{ijk}	dissipation rate of triple-velocity products, $\langle u_i u_j u_k \rangle$
$\varepsilon_{i\theta}$	dissipation rate of the turbulent heat flux, $\langle u_i \theta \rangle$
$\varepsilon_{ij\theta}$	dissipation rate of third moments of velocity and temperature, $\langle u_i u_j \theta \rangle$
θ	fluctuating component of temperature
μ	dynamic viscosity
μ_t	turbulent viscosity ($= C_\mu \rho k^2/\varepsilon$)
ν	kinematic viscosity
ρ	density of the fluid
τ	shear stress
Φ_{ij}	pressure-strain redistribution for Reynolds stresses, $\langle u_i u_j \rangle$
$\Phi_{ij,w}$	near-wall effects in the pressure-strain redistribution for Reynolds stresses, $\langle u_i u_j \rangle$
Φ_{ijk}	pressure-stress correlation for triple-velocity products, $\langle u_i u_j u_k \rangle$
$\Phi_{ijk,w}$	pressure-stress correlation of the near-wall low-Reynolds number effect for triple-velocity products, $\langle u_i u_j u_k \rangle$
$\Phi_{i\theta}$	pressure-heat flux correlation for $\langle u_i \theta \rangle$
$\Phi_{i\theta,w}$	near-wall effects in the pressure-heat flux correlation for $\langle u_i \theta \rangle$
$\Phi_{ij\theta}$	pressure-heat flux correlation for the triple products, $\langle u_i u_j \theta \rangle$

Subscripts

i,j,k,ℓ,m,n	tensor notations
w	wall values
IN	inlet station (x/H = −4) condition

Symbols

< >	time-averaged values

INTRODUCTION

Separation and recirculation of flow is encountered in a vast array of engineering applications. This phenomenon of flow separation and recirculation associates itself with higher turbulence levels which not only render the flow greater analytical complexity but also result in augmenting its heat transfer and momentum aspects considerably.

Current research in this area is mainly limited to experimental measurements of the hydrodynamic characteristics along with the heat transfer coefficients in the flow domain. Computation of the temperature field in the flow domain entails the solution of the time averaged temperature equation containing the turbulence fluctuating velocity-temperature products. These second moments or double products are correlated in terms of Boussinesq's isotropic viscosity and the turbulent Prandtl number in order to close and solve the temperature equation. However, as pointed out by Launder and Samaraweera,[1] the second-moment model is more preferable because turbulent interactions which generate the turbulence stresses and heat fluxes can be treated exactly. They applied an algebraic second-moment turbulence closure to heat and mass transport in thin shear flows and obtained good results.

Algebraic turbulence scalar-velocity models containing the curvature and gravitational effects have been proposed and used by Tahry et al.[2] and Gibson[3] for predicting the heat fluxes in turbulent shear flows and boundary layer flows.

The third moments, which are responsible for the diffusive transport of the second moments, attain greater significance in recirculating flows, as pointed out by Chandrsuda and Bradshaw[4]; these also have not been given much attention and, therefore, need to be examined in greater detail in order to fully understand and comprehend the turbulent transport mechanisms.

Owing to the relative complexity commonly encountered in recirculating flows, experimental measurements of the second and third moments, hence, pose a formidable challenge. Ota and Kon[5] report uncertainties of up to 50% in their measurements of second moments in the reattachment region using conventional hot wire instruments; similar measurements were made by Seki et al.[6] Vogel and Eaton[7] and Adams et al.[8] made extensive measurements of the thermal and mass fluxes using LDAs. Experimental information on the behavior of the triple products of scalar-velocity fluctuations is almost nonexistent. Andreopoulos and Bradshaw[9], however, present the variation of the triple products for a flow over a boundary layer using constant temperature anemometers and Antonia[10] presents those for a plane jet.

The study undertaken and presented here solves the flow into a backward-facing step geometry. After obtaining a good agreement for the hydrodynamic parameters, the thermal variables are solved. The transport equations of the turbulence scalar-velocity products, $\langle u_i\theta \rangle$ and $\langle u_i u_j \theta \rangle$, are developed and solved to obtain their profiles in recirculating and redeveloping flow regions beyond the step.

MATHEMATICAL MODELS

The transport equation for the Reynolds stresses is given as

$$\frac{\partial}{\partial x_k}\left(U_k \langle u_i u_j \rangle\right) = P_{ij} - \varepsilon_{ij} + \phi_{ij} + \phi_{ij,w} + D_{ij} \qquad (1)$$

where P_{ij}, ϕ_{ij} , and $\phi_{ij,w}$, respectively, represent the production, pressure-strain, and the wall correlation for pressure-strain rates. These are all defined by Launder et al.[11]

The diffusion rate, D_{ij}, contains the terms given as follows

$$D_{ij} = -\frac{\partial}{\partial x_k}\left[\langle u_i u_j u_k\rangle + \frac{\langle u_i p\rangle}{\rho}\delta_{jk} + \frac{\langle u_j p\rangle}{\rho}\delta_{ik}\right.$$

$$\left. - \nu\left(\frac{\partial\langle u_i u_j\rangle}{\partial x_k} + \left\langle u_j \frac{\partial u_k}{\partial x_i}\right\rangle + \left\langle u_i \frac{\partial u_k}{\partial x_j}\right\rangle\right)\right] \qquad (2)$$

Since the diffusion rate of the Reynolds stresses is governed by the gradient of the third moments $\langle u_i u_j u_k\rangle$, it becomes necessary to evaluate the third moments accurately.

The third moments, $\langle u_i u_j u_k\rangle$, can be evaluated by formulating their transport equation as

$$\frac{\partial}{\partial x_\ell}\left(U_\ell \langle u_i u_j u_k\rangle\right) = -\left(\langle u_i u_j u_\ell\rangle \frac{\partial U_k}{\partial x_\ell} + \langle u_j u_k u_\ell\rangle \frac{\partial U_i}{\partial x_\ell} + \langle u_k u_i u_\ell\rangle \frac{\partial U_j}{\partial x_\ell}\right)$$

(I)

$$+ \left(\langle u_i u_j\rangle \frac{\partial\langle u_k u_\ell\rangle}{\partial x_\ell} + \langle u_j u_k\rangle \frac{\partial\langle u_i u_\ell\rangle}{\partial x_\ell} + \langle u_k u_i\rangle \frac{\partial\langle u_j u_\ell\rangle}{\partial x_\ell}\right)$$

(II)

$$- \left(\left\langle u_i u_j \frac{\partial u_k u_\ell}{\partial x_\ell}\right\rangle + \left\langle u_j u_k \frac{\partial u_i u_\ell}{\partial x_\ell}\right\rangle + \left\langle u_k u_i \frac{\partial u_j u_\ell}{\partial x_\ell}\right\rangle\right)$$

(III) (3)

$$- \frac{1}{\rho}\left(\left\langle u_i u_j \frac{\partial p}{\partial x_k}\right\rangle + \left\langle u_j u_k \frac{\partial p}{\partial x_i}\right\rangle + \left\langle u_k u_i \frac{\partial p}{\partial x_j}\right\rangle\right)$$

(IV)

$$+ \left\langle u_i u_j \frac{\partial}{\partial x_\ell}\left[\nu\left(\frac{\partial u_k}{\partial x_\ell} + \frac{\partial u_\ell}{\partial x_k}\right)\right]\right\rangle$$

$$+ \left\langle u_j u_k \frac{\partial}{\partial x_\ell}\left[\nu\left(\frac{\partial u_i}{\partial x_\ell} + \frac{\partial u_\ell}{\partial x_i}\right)\right]\right\rangle$$

$$+ \left\langle u_k u_i \frac{\partial}{\partial x_\ell}\left[\nu\left(\frac{\partial u_j}{\partial u_\ell} + \frac{\partial u_\ell}{\partial x_j}\right)\right]\right\rangle$$

(V)

In order to account for the viscous effects that are predominant near the wall, a low-Reynolds number modification needs to be incorporated in the transport equations of the third moments.

The theory behind this low-Reynolds number modeling is based upon the existence of the viscous sublayer, the buffer layer and the fully turbulent core in the near-wall region. The profiles of the energy dissipation rate ε are accounted for in all three layers, and the pressure-stress correlation is modified accordingly.

Finally, the transport equation for $\langle u_i u_j u_k \rangle$ containing the low-Reynolds number effect is given as

$$\frac{\partial}{\partial x_\ell}(U_\ell \langle u_i u_j u_k \rangle) = P_{ijk_1} + P_{ijk_2} + \phi_{ijk} + \phi_{ijk,w} + \varepsilon_{ijk} + D_{ijk} \tag{4}$$

where

$P_{ijk,1} \equiv$ production due to mean strains

$$= -C_g(\langle u_i u_j u_\ell \rangle \frac{\partial U_k}{\partial x_\ell} + \langle u_j u_k u_\ell \rangle \frac{\partial U_i}{\partial x_\ell} + \langle u_k u_i u_\ell \rangle \frac{\partial U_j}{\partial x_\ell}) \tag{5}$$

$P_{ijk,2} \equiv$ Production due to Reynolds stresses interacting with their gradients

$$= -(\langle u_k u_\ell \rangle \frac{\partial \langle u_i u_j \rangle}{\partial x_\ell} + \langle u_i u_\ell \rangle \frac{\partial \langle u_j u_k \rangle}{\partial x_\ell} + \langle u_j u_\ell \rangle \frac{\partial \langle u_k u_i \rangle}{\partial x_\ell}) \tag{6}$$

$\phi_{ijk} + \phi_{ijk,w} \equiv$ Pressure-stress term including the low-Reynolds number effect.

$$= C_\gamma \frac{\langle u_i u_j u_k \rangle}{k} \{\varepsilon + \max [C_{\gamma w} \frac{k^{3/2}}{C_\ell y} , 2\nu (\frac{\partial k^{1/2}}{\partial y})^2]\} \quad (7)$$

$\varepsilon_{ijk} \equiv$ Dissipation due to viscous action

$$= C_{\varepsilon\gamma} \frac{2}{3} (\delta_{ij} + \delta_{jk} + \delta_{ki}) \varepsilon k^{1/2} \quad (8)$$

and $D_{ijk} \equiv$ Diffusion rate

$$= \frac{\partial}{\partial x_\ell} (\nu \frac{\partial}{\partial x_\ell} \langle u_i u_j u_k \rangle) \quad (9)$$

The values of the constants are listed in Table 1.

The model given by Eq. (7) was originally tested by Amano et al.[12] where it was shown that the addition of the bracketed term remarkably improves the prediction of $\langle u_i u_j u_k \rangle$ in the near-wall region.

Table 1. Recommended values for the constants used in turbulence modeling.

C_g	C_γ	$C_{\gamma w}$	$C_{\varepsilon\gamma}$	$C_{i\theta,1}$	$C_{i\theta,2}$	C_{IT}	C_{2T}	$C_{\theta\gamma}$	$C_{\theta\varepsilon}$
1.0	3.0	8.0	0.10	3.2	0.5	0.313	0.156	6.0	0.10

The Reynolds-stress closure is consolidated by incorporating the equations of k and ε and the transport equations of the third moments, $\langle u_i u_j u_k \rangle$, into the Reynolds-stress equations.

The temperature field is obtained by solving the time-averaged temperature equation given as

$$\frac{\partial U_j T}{\partial x_j} = \frac{1}{\rho} \frac{\partial}{\partial x_j} [(\frac{\mu}{Pr} + \frac{\mu_t}{Pr_t}) \frac{\partial T}{\partial x_j}] \quad (10)$$

where Pr_t = turbulent Prandtl number (= 0.9).

In order to obtain the second moments of temperature, $\langle u_i\theta \rangle$, their transport equation is formulated and various terms in it are then approximated through closures.

The transport equation for $\langle u_i\theta \rangle$ after neglecting insignificant terms can be written as

$$\frac{\partial}{\partial x_j}(U_j \langle u_i\theta \rangle) = -\left[\langle u_i u_j \rangle \frac{\partial T}{\partial x_j} + \langle u_j\theta \rangle \frac{\partial U_i}{\partial x_j}\right] \qquad \text{(I)}$$

$$+ \frac{\partial}{\partial x_j}\left[(\alpha + \nu)\frac{\partial}{\partial x_j}\langle u_i\theta \rangle - \langle u_i u_j \theta \rangle\right] \qquad \text{(II)}$$

$$+ \left\langle \frac{p}{\rho}\frac{\partial \theta}{\partial x_i} \right\rangle - (\alpha + \nu)\left\langle \frac{\partial \theta}{\partial x_j}\frac{\partial u_i}{\partial x_j} \right\rangle \qquad \text{(III)} \quad \text{(IV)} \qquad (11)$$

which can be written as

$$\frac{\partial}{\partial x_j}(U_j \langle u_i\theta \rangle) = P_{i\theta} + D_{i\theta} + \phi_{i\theta} - \varepsilon_{i\theta} \qquad (12)$$

where

$P_{i\theta} \equiv$ Production rate of $\langle u_i\theta \rangle$

$D_{i\theta} \equiv$ Diffusion rate of $\langle u_i\theta \rangle$

$\phi_{i\theta} \equiv$ Pressure-heat flux effects

and $\varepsilon_{i\theta} \equiv$ Dissipation of $\langle u_i\theta . \rangle$

$P_{i\theta}$ (Term (I)) needs no further approximation since it is explicit in its character.

The diffusive rates which are comprised of the triple products $\langle u_i u_j \theta \rangle$ are modeled by decomposing the third moments into the second moments as shown by Launder,[13]

$$\langle u_i u_j \theta \rangle = - 0.15 \left(2 \frac{k}{\varepsilon}\right) \langle u_j u_\ell \rangle \frac{\partial \langle u_i \theta \rangle}{\partial x_\ell}] \tag{13}$$

Thus, the diffusion is now given as

$$D_{i\theta} = \frac{\partial}{\partial x_j} [(\alpha + \nu) \frac{\partial \langle u_i \theta \rangle}{\partial x_j} + \frac{0.30k}{\varepsilon} \langle u_j u_\ell \rangle \frac{\partial \langle u_i \theta \rangle}{\partial x_\ell}] \tag{14}$$

The pressure-heat flux term can be expressed as[13]

$$\phi_{i\theta} = - C_{i\theta,1} \frac{\varepsilon}{k} \langle u_i \theta \rangle + C_{i\theta,2} \langle u_\ell \theta \rangle \frac{\partial U_i}{\partial x_\ell} \tag{15}$$

The dissipation rate, $\varepsilon_{i\theta}$, is assumed to be negligible in accordance with the assumptions made in the Reynolds-stress closures. Launder and Samaraweera[1] also propose a near-wall correction term $\phi_{i\theta,w}$ to be added to the pressure-heat flux term, $\phi_{i\theta}$, which is given as

$$\phi_{i\theta,w} = [- 0.10 \frac{\varepsilon}{k} \langle u_i \theta \rangle - 0.02 \langle u_i \theta \rangle \{4 \frac{\partial U_i}{\partial x_\ell} - \frac{\partial U_\ell}{\partial x_i}\}] \frac{k^{3/2}}{\varepsilon x_n} \tag{16}$$

where x_n is the distance from the wall.

Algebraic expressions to model the second moments are also developed by Launder [14] which after neglecting the gravitational effects can be expressed as

$$- \langle u_i \theta \rangle = C_{1T} \frac{k}{\varepsilon} \langle u_k u_i \rangle \frac{\partial T}{\partial x_k} + C_{2T} \frac{k}{\varepsilon} \langle u_k \theta \rangle \frac{\partial U_i}{\partial x_k} \tag{17}$$

In order to evaluate the third moments of temperature, $\langle u_i u_j \theta \rangle$, it is necessary to formulate their transport equation. This is given as follows:

$$\frac{\partial}{\partial x_k}\left(U_k \langle u_i u_j \theta \rangle\right) = -\Big[\langle u_i u_j u_k \rangle \frac{\partial T}{\partial x_k} + \langle u_j u_k \theta \rangle \frac{\partial U_i}{\partial x_k} + \langle u_k u_i \theta \rangle \frac{\partial U_j}{\partial x_k}\Big]$$

(I)

$$-\Big[\langle u_i u_j \frac{\partial}{\partial x_k}(u_k\theta - \langle u_k\theta\rangle)\rangle + \langle u_i\theta \frac{\partial}{\partial x_k}(u_j u_k - \langle u_j u_k\rangle)\rangle$$

$$+ \langle u_j\theta \frac{\partial}{\partial x_k}(u_k u_i - \langle u_k u_i\rangle)\rangle\Big]$$

(II)

$$-\Big[\langle \frac{u_i\theta}{\rho}\frac{\partial p}{\partial x_j}\rangle + \langle \frac{u_j\theta}{\rho}\frac{\partial p}{\partial x_i}\rangle\Big]$$

(III)

$$-\Big[\langle u_i u_j \frac{\partial}{\partial x_k}(\alpha \frac{\partial\theta}{\partial x_k})\rangle + \langle u_i\theta \frac{\partial}{\partial x_k}(\frac{\mu}{\rho}\frac{\partial u_j}{\partial x_k})\rangle + \langle u_j\theta \frac{\partial}{\partial x_k}(\frac{\mu}{\rho}\frac{\partial u_i}{\partial x_k})\rangle\Big] \quad (18)$$

(IV)

where

Term (I) = Production due to mean strain rate and temperature gradients

Term (II) = Production rate due to the interaction of the Reynolds stresses and their gradients with the heat flux components $\langle u_i\theta\rangle$ and $\langle u_j\theta\rangle$.

Term (III) = Pressure-heat flux effects

Term (IV) = Diffusion and dissipative effects due to molecular viscosity.

In closing the above equation, Term (I) needs no further approximation since it is rather explicit in its form. Term (II) can be rearranged and written as:

$$\text{Term (II)} = \langle u_i u_j \rangle \frac{\partial \langle u_k \theta \rangle}{\partial x_k} + \langle u_i \theta \rangle \frac{\partial \langle u_j u_k \rangle}{\partial x_k} + \langle u_j \theta \rangle \frac{\partial \langle u_k u_i \rangle}{\partial x_k} - \frac{\partial}{\partial x_k} (\langle u_i u_j u_k \theta \rangle) \tag{19}$$

The quadruple term is assumed to be Gaussian and can be split up as

$$\langle u_i u_j u_k \theta \rangle = \langle u_i u_j \rangle \cdot \langle u_k \theta \rangle + \langle u_j u_k \rangle \cdot \langle u_i \theta \rangle + \langle u_k u_i \rangle \cdot \langle u_j \theta \rangle \tag{20}$$

Differentiating Eq. (20) with respect to x_k and substituting the result in Eq. (19) yields

$$\text{Term (II)} = - \langle u_j u_k \rangle \frac{\partial \langle u_i \theta \rangle}{\partial x_k} - \langle u_k u_i \rangle \frac{\partial \langle u_j \theta \rangle}{\partial x_k} - \langle u_k \theta \rangle \frac{\partial \langle u_i u_j \rangle}{\partial x_k} \tag{21}$$

The pressure-heat flux effects of Term (III) can be approximated by first forming the Poisson equation for fluctuating pressure and then approximating the term by a simplified closure.

The Poisson equation for fluctuating pressure is

$$\frac{1}{\rho} \frac{\partial p}{\partial x_\ell} = - \int \{ \frac{\partial^2}{\partial x_\ell \partial x_m} (u_\ell u_m - \langle u_\ell u_m \rangle) + \frac{2 \partial u_m}{\partial x_\ell} \frac{\partial U_\ell}{\partial x_m} \} \, dx_\ell \tag{22}$$

After multiplying $u_n \theta$ and time averaging with suitable approximation, this may be given as

$$\langle \frac{u_n \theta}{\rho} \frac{\partial p}{\partial x_\ell} \rangle \simeq - C_1 \langle u_n u_\ell \theta \rangle \frac{\varepsilon}{k} + C_2 \langle u_m u_n \theta \rangle \frac{\partial U_\ell}{\partial x_m} \tag{23}$$

where C_1 and C_2 are arbitrary constants.

Based upon this approximation, Term (III) is thus correlated as

$$\text{Term (III)} = - \langle \frac{u_i \theta}{\rho} \frac{\partial p}{\partial x_j} \rangle - \langle \frac{u_j \theta}{\rho} \frac{\partial p}{\partial x_i} \rangle \simeq C_1 \langle u_i u_j \theta \rangle \frac{\varepsilon}{k}$$

$$+ C_2 [\langle u_j u_k \theta \rangle \frac{\partial U_i}{\partial x_k} + \langle u_k u_i \theta \rangle \frac{\partial U_j}{\partial x_k}] = C_{\theta\gamma} \langle u_i u_j \theta \rangle \frac{\varepsilon}{k} \tag{24}$$

where the second term in Eq. (24) is merged into Term (I) and the coefficient $C_{\theta\gamma}$ adjusted accordingly. (The value of $C_{\theta\gamma}$ has to be determined by parametric testing.)

Term (IV) contains the diffusive and dissipative effects due to molecular viscosity. This may be rearranged as

$$\text{Term (IV)} = (\alpha + 2\nu) \frac{\partial}{\partial x_k} \{\frac{\partial}{\partial x_k} \langle u_i u_j \theta \rangle\}$$

$$- \alpha \left[2 \left\langle \frac{\partial \theta}{\partial x_k} \frac{\partial u_i u_j}{\partial x_k} \right\rangle + \left\langle \frac{\theta \partial^2 u_i u_j}{\partial x_k^2}^* \right\rangle\right]$$

$$- \nu \left[2 \left\langle \frac{\partial u_i}{\partial x_k} \frac{\partial u_j \theta}{\partial x_k} \right\rangle + \left\langle \frac{u_i \partial^2 u_j \theta}{\partial x_k^2}^* \right\rangle\right]$$

$$- \nu \left[2 \left\langle \frac{\partial u_j}{\partial x_k} \frac{\partial u_i \theta}{\partial x_k} \right\rangle + \left\langle u_j \frac{\partial^2 u_i \theta}{\partial x_k^2}^* \right\rangle\right] \qquad (25)$$

The first term in Eq. (25) represents the laminar diffusion while the rest of the terms express the dissipative effects. The terms with the asterisk (*) consist of second derivatives of the second moments and are assumed to be negligible. The effect of neglecting the terms is adjusted by manipulating the value of the empirical coefficients used in the modeling.

The dissipative effects of Term (IV) in Eq. (25) are further assumed to be

$$\varepsilon_{ij\theta} = C_{\theta\varepsilon} \frac{k}{\varepsilon} \left(\langle u_k \theta \rangle \frac{\partial \varepsilon}{\partial x_k}\right) \qquad (26)$$

The final form of the transport equation for $\langle u_i u_j \theta \rangle$ is now written as

$$\frac{\partial}{\partial x_k} \left(U_k \langle u_i u_j \theta \rangle\right) = P_{ij\theta,1} + P_{ij\theta,2} + D_{ij\theta} + \Phi_{ij\theta} - \varepsilon_{ij\theta} \qquad (27)$$

where

$$P_{ij\theta,1} = - [\langle u_i u_j u_k \rangle \frac{\partial T}{\partial x_k} + \langle u_j u_k \theta \rangle \frac{\partial U_i}{\partial x_k} + \langle u_k u_i \theta \rangle \frac{\partial U_j}{\partial x_k}] \tag{28}$$

$$P_{ij\theta,2} = - [\langle u_j u_k \rangle \frac{\partial \langle u_i \theta \rangle}{\partial x_k} + \langle u_k u_i \rangle \frac{\partial \langle u_j \theta \rangle}{\partial x_k} + \langle u_k \theta \rangle \frac{\partial \langle u_i u_j \rangle}{\partial x_k}] \tag{29}$$

$$D_{ij\theta} = \frac{\partial}{\partial x_k} [(\alpha + 2\nu) \frac{\partial}{\partial x_k} \langle u_i u_j \theta \rangle] \tag{30}$$

$$\Phi_{ij\theta} = - C_{\theta\gamma} \frac{\varepsilon}{k} \langle u_i u_j \theta \rangle \tag{31}$$

and

$$\varepsilon_{ij\theta} = C_{\theta\varepsilon} \frac{\varepsilon}{k} \langle u_k \theta \rangle \frac{\partial \varepsilon}{\partial x_k} \tag{32}$$

In addition to the transport equation for $\langle u_i u_j \theta \rangle$, the existing algebraic correlations are:

1. Launder[13]

$$\langle u_i u_j \theta \rangle = - 0.10 \frac{2k}{\varepsilon} (\langle u_i u_\ell \rangle \frac{\partial \langle u_j \theta \rangle}{\partial x_\ell} + \langle u_j u_\ell \rangle \frac{\partial \langle u_i \theta \rangle}{\partial x_\ell}) \tag{33}$$

2. Wyngaard and Cote[15]

$$\langle u_i u_j \theta \rangle = - 0.15 \frac{2k}{\varepsilon} (\langle u_i u_\ell \rangle \frac{\partial \langle u_j \theta \rangle}{\partial x_\ell}) \tag{34}$$

3. Donaldson et al.[16]

$$\langle u_i u_j \theta \rangle = - 0.10 \frac{4k^2}{\varepsilon} (\frac{\partial \langle u_i \theta \rangle}{\partial x_j} + \frac{\partial \langle u_j \theta \rangle}{\partial x_i}) \tag{35}$$

SOLUTION PROCEDURE

The computation was performed using a 62 x 62 variable grid mesh with the grid expanding linearly at the rate of 2% in the axial direction and at 3% in

the transverse direction from the step wall. The details of this adoption is discussed in the next section.

Computations of the transport equations described in the preceding section is achieved by using a finite volume method.[12] The iterative procedure is terminated when the maximum value of the relative residual sources of U, V, and mass balance falls below 1%. However, the computations of the triple products are terminated when the relative residual sources fall below 3×10^{-8} for $\langle u_i u_j u_k \rangle$ and 5.0×10^{-9} for $\langle u_i u_j \theta \rangle$.

This complete process of solving the momentum, temperature and their related turbulence products equations takes about 60 minutes of CPU time on a UNIVAC 1100 computer. For the solution of the transport equation of the temperature and temperature associated moments, boundary conditions had to be specified at the solid wall and the outflow section of the channel.

For the temperature equation, a constant heat flux of 130 W/m was applied along the wall downstream of the step. This heat flux was introduced into the solution domain by supplementing the source term at the wall adjacent cell for the temperature equation with this heat flux.

The wall boundary condition for $\langle u\theta \rangle$ and $\langle v\theta \rangle$ is based upon the fact that at the wall,

$$\langle u\theta \rangle = \langle v\theta \rangle = 0.0. \tag{36}$$

Therefore, the value of $\langle v\theta \rangle$ at the wall adjacent node is fixed by the interpolation between the wall and the node next to the wall adjacent node. The value of $\langle u\theta \rangle$ at the wall adjacent node is set equal to minus twice the value of $\langle v\theta \rangle$ at this node, as pointed out by Launder.[13]

Since the scalar-velocity products $\langle u_i u_j \theta \rangle$ fall to zero at the wall, their near-wall values, hence, have been accordingly made very small such that they tend to zero at the wall.

As mentioned in Amano et al.[12] the third moments are fairly stable and seem to be affected very little by the choice of the wall boundary treatment. At the outflow section which is located at a distance of 60H from the step, a parabolic boundary condition is applied thereby causing the streamwise gradient of all the parameters (except T) to vanish.

The temperature distribution at the outflow section is prescribed in accordance with Kays and Crawford[17] wherein

$$\frac{dT}{dx} = \frac{2q_w''}{\rho c_p U D_c} \tag{37}$$

RESULTS AND DISCUSSION

Figure 1 depicts the flow configuration inside a backward-facing step geometry. The shear flow separates at the edge of the step and forms a separated shear layer which causes a part of the fluid to recirculate and the rest to continue to flow downstream contributing to the stabilization of the flow through the formation of a boundary layer in the redeveloping region.

Experimental data of Driver and Seegmiller[18] has been used for comparison with the computational results.

Figures 2 and 3 compare the skin friction coefficient and pressure coefficient, respectively along the wall downstream of the step with the experimental data. Computations have been performed with several different grid systems ranging from 32 x 32 to 62 x 62. It is shown in both figures that a fair grid independent status is attained with the grid system finer than 52 x 52. Thus the grid of 62 x 62 has been adopted in this study. It is further noticed that agreement between the computation and the data is fairly reasonable.

Figure 4 compares the mean velocity profiles and Figs. 5, 6, and 7, respectively, compare the Reynolds stresses $\langle u^2 \rangle$, $\langle v^2 \rangle$ and $\langle uv \rangle$ with the experimental data. The agreement with the experimental data is generally satisfactory.

In Figs. 8-11 triple velocity products are compared with the experimental data of Driver and Seegmiller.[18] The results are also compared with several algebraic models in the literature. As shown in these figures, the levels of the triple-velocity products are always higher in the shear layer with employing the transport models than with the algebraic correlations. Thus, the transport model gives more realistic results in comparison with the data. The reason for this is that the convective and diffusive effects are accounted for through the reattaching shear layer with the transport model whereas these effects are mostly neglected in the algebraic correlations.

Since the physical properties of the fluid are assumed to be invariant with temperature, hydrodynamic aspects of the flow are independent of its thermal characteristics. Therefore, the temperature along with its second and third moments are obtained using the converged stored values of the hydrodynamic parameters.

Figure 12 shows the nondimensionalized temperature profiles downstream of the step. These results, comparing the data taken by Eason and Vogel,[19] show very satisfactory agreement.

Figures 13 and 14 show respectively the nondimensionalized heat flux $\langle u\theta \rangle$ and $\langle v\theta \rangle$ profiles downstream of the step. Results obtained by the solution of their transport equation (Eq. 12) are compared with the results obtained by the algebraic correlation (Eq. 17). It is seen that the overall agreement between the results obtained by the transport equations and the

algebraic equations is quite reasonable. It is further noticed that the agreement of $\langle v\theta \rangle$ is very good in the shear layer but closer to the wall the algebraic model fails to diminish the levels of $\langle v\theta \rangle$. On the contrary, the algebraic models tend to make $\langle v\theta \rangle$ go to infinity. The transport equations, however, with the proper imposition of the boundary conditions give more realistic results.

Profiles of the triple products of velocity and temperature $\langle u_i u_j \theta \rangle$ are shown in Figs. 15-17. Results by solving the transport equations for $\langle u_i u_j \theta \rangle$ (Eq. 27) are compared with results obtained by the algebraic correlations for $\langle u_i u_j \theta \rangle$ by Launder[13], Wyngaard and Cote,[15] and Donaldson et al.,[16]: Eqs. (33), (34) and (35), respectively.

There is no experimental data available for validation and comparison owing to the relative complexity involved in the measurements of double and triple products ($\langle u_i \theta \rangle$ and $\langle u_i u_j \theta \rangle$) inside wall bounded recirculating flows.

Figure 15 shows the nondimensionalized profiles for $\langle uu\theta \rangle$. Predictions by the three algebraic correlations seem to be very close to one another. The predictions by the transport equation are the highest particularly in the shear layer. Although the three algebraic correlations predict similar results, the model of Launder[13] predicts the highest values and that of Donaldson et al.[16] predicts the lowest. However, the difference among the predictions is very small, particularly near the reattachment region and beyond.

Figure 16 depicts the profiles of $\langle uv\theta \rangle$. The prediction by the algebraic models and the transport equations are very close. The model of Donaldson et al.[16] gives the highest values whereas the model of Wyngaard and Cote[15] gives the lowest. Predictions by the transport equations are somewhat intermediate.

Figure 17 shows the profiles for $\langle vv\theta \rangle$ obtained by the transport equation (Eq. 27) and the above mentioned algebraic correlations. The predictions by the model of Donaldson et al.[16] predominate over the others, and the transport equations give the smallest values. The predictions by the model of Launder[15] show smaller than those by the model of Donaldson et al.,[16] but larger than those of Wyngaard and Cote's[15] model. The differences between the predictions become smaller with increasing distance downstream from the step.

It is generally seen that the predictions by the algebraic models and the transport equations have similar trends and the difference between their predictions becomes smaller in the reattachment and redeveloping regions. However, the near-wall values of all the models are rather high. It is possible to treat the near-wall values of $\langle u_i u_j \theta \rangle$ through the incorporation of a suitable low-Reynolds number model in their transport equations. But it is not easy to modify the algebraic equations to accommodate this. It is anticipated that the transport equations of the third moments with a low-Reynolds number model would be superior to other algebraic correlations.

CONCLUSIONS

The second-and third-order closures for the hydrodynamic characteristics are extended to the scalar (temperature) field wherein transport equations for the fluctuating velocity-temperature moments are developed and solved for the flow over a backward-facing step.

Prediction for $\langle u_i \theta \rangle$ and $\langle u_i u_j \theta \rangle$ obtained by solving their transport equations are compared with algebraic models and the superiority and potentiality of the transport equations for these double and triple products are demonstrated.

REFERENCES

1. Launder, B. E., and Samaraweera, D. S. A., "Application of a Second Moment Turbulence Closure to Heat and Mass Transport in Thin Shear Flows, I. Two-Dimensional Transport," International Journal of Heat and Mass Transfer, Vol. 22, 1979, pp. 1631-1643.

2. Tahry, S. E., Gosman, A. D., and Launder, B. E., "The Two- and Three-Dimensional Dispersal of a Passive Scalar in a Turbulent Boundary Layer," International Journal of Heat and Mass Transfer, Vol. 24, 1981, pp. 35-46.

3. Gibson, M. M., "An Algebraic Stress and Heat-Flux Model for Turbulent Shear Flow with Streamline Curvature," International Journal of Heat and Mass Transfer, Vol. 21, 1978, pp. 1609-1617.

4. Chandrsuda, C. and Bradshaw, P., "Turbulence Structure of a Reattaching Mixing Layer," Journal of Fluid Mechanics, Vol. 110, 1981, pp. 171-194.

5. Ota, T., and Kon, N., "Turbulent Transfer of Momentum and Heat in a Separated and Reattached Flow over a Blunt Flat Plate," Journal of Heat Transfer, Vol. 102, 1980, pp. 749-754.

6. Seki, N., Fukusako, S., and Hirata, T., "Turbulent Fluctuations and Heat Transfer for Separated Flow Associated with a Double Step at Entrance to an Enlarged Flat Duct," Journal of Heat Transfer, Nov., 1976, pp. 588-593.

7. Vogel, J. C., and Eaton, J. K., "Heat Transfer and Fluid Mechanics Measurements in the Turbulent Reattaching Flow Behind a Backward Facing Step," Report MD-44, August 1984, Stanford University.

8. Adams, E. W., Johnston, J. P., and Eaton, J. K., "Experiments on the Structure of Turbulent Reattaching Flow," Report MD-43, May 1984, Stanford University.

9. Andreopoulos, J., and Bradshaw, P., "The Thermal Boundary Layer Far Downstream of a Spanwise Line Source of Heat," Journal of Heat Transfer, Vol. 102, 1980, pp 755-760.

10. Antonia, R. A., "On a Heat Transport Model for a Turbulent Plane Jet," International Journal of Heat and Mass Transfer, Vol. 28, No. 10, 1985, pp. 1805-1812.

11. Launder, B. E., Reece, G. J., and Rodi, W., "Progress in the Development of a Reynolds Stress Turbulence Closure," Journal of Fluid Mechanics, Vol. 68, 1975, pp. 537-566.

12. Amano, R. S., Goel, P., and Chai, J. C., "Turbulence Energy and Diffusion Transport in a Separating and Reattaching Flow," AIAA Journal, to appear in 1987.

13. Launder, B. E., "Heat and Mass Transport," in Turbulence - Topics on Applied Physics, (edited by P. Bradshaw), Vol. 12, Chapter 6, 1976.

14. Launder, B. E., "On the Effects of a Gravitational Field on the Turbulent Transport of Heat and Momentum," Journal of Fluid Mechanics, Vol. 67, Part 3, 1975, pp. 569-581.

15. Wyngaard, J. C., Cote, O. R., and Rao, K.S., "Modeling the Atmospheric Boundary Layer," Adv. Geophysics, Vol. 18A, 1974, pp. 193-211.

16. Donaldson, C. D. P., Sullivan, R. D., and Rosenbaum, H., "A Theoretical Study of the Generation of Atmospheric-Clear Air Turbulence," AIAA Journal, Vol. 10, 1972, pp. 162-170.

17. Kays, W. M., and Crawford, M. E., Convective Heat and Mass Transfer, McGraw Hill, Second Edition, 1980.

18. Driver, D. M., and Seegmiller, H. L., "Features of a Reattaching Turbulent Shear Layer in Divergent Channel Flow," AIAA Journal, Vol. 23, No. 2, 1985, pp. 163-171.

19. Vogel, J. C. and Eaton, J. K., "Heat Transfer and Fluid Mechanics Measurements in the Turbulent Reattaching Flow Behind a Backward-Facing Step," Report MD-44, 1984, Standford University.

FIGURE CAPTIONS

Figure 1 Solution domain -- Backward-facing geometry with the separating, recirculation and redeveloping regions.

Figure 2 Skin friction coefficient along the bottom wall downstream on the step.

Figure 3 Pressure coefficient along the bottom wall downstream of the step.

Figure 4 U-velocity profiles downstream of the step.

Figure 5 <uu>-profiles downstream of the step.

Figure 6 <vv>-profiles downstream of the step.

Figure 7 <uv>-profiles downstream of the step.

Figure 8 <uuu>-profiles downstream of the step.

Figure 9 <uuv>-profiles downstream of the step.

Figure 10 <uvv>-profiles downstream of the step.

Figure 11 <vvv>-profiles downstream of the step.

Figure 12 T-profiles downstream of the step.

Figure 13 <uθ>-profiles downstream of the step.

Figure 14 <vθ>-profiles downstream of the step.

Figure 15 <uuθ>-profiles downstream of the step.

Figure 16 <uvθ>-profiles downstream of the step.

Figure 17 <vvθ>-profiles downstream of the step.

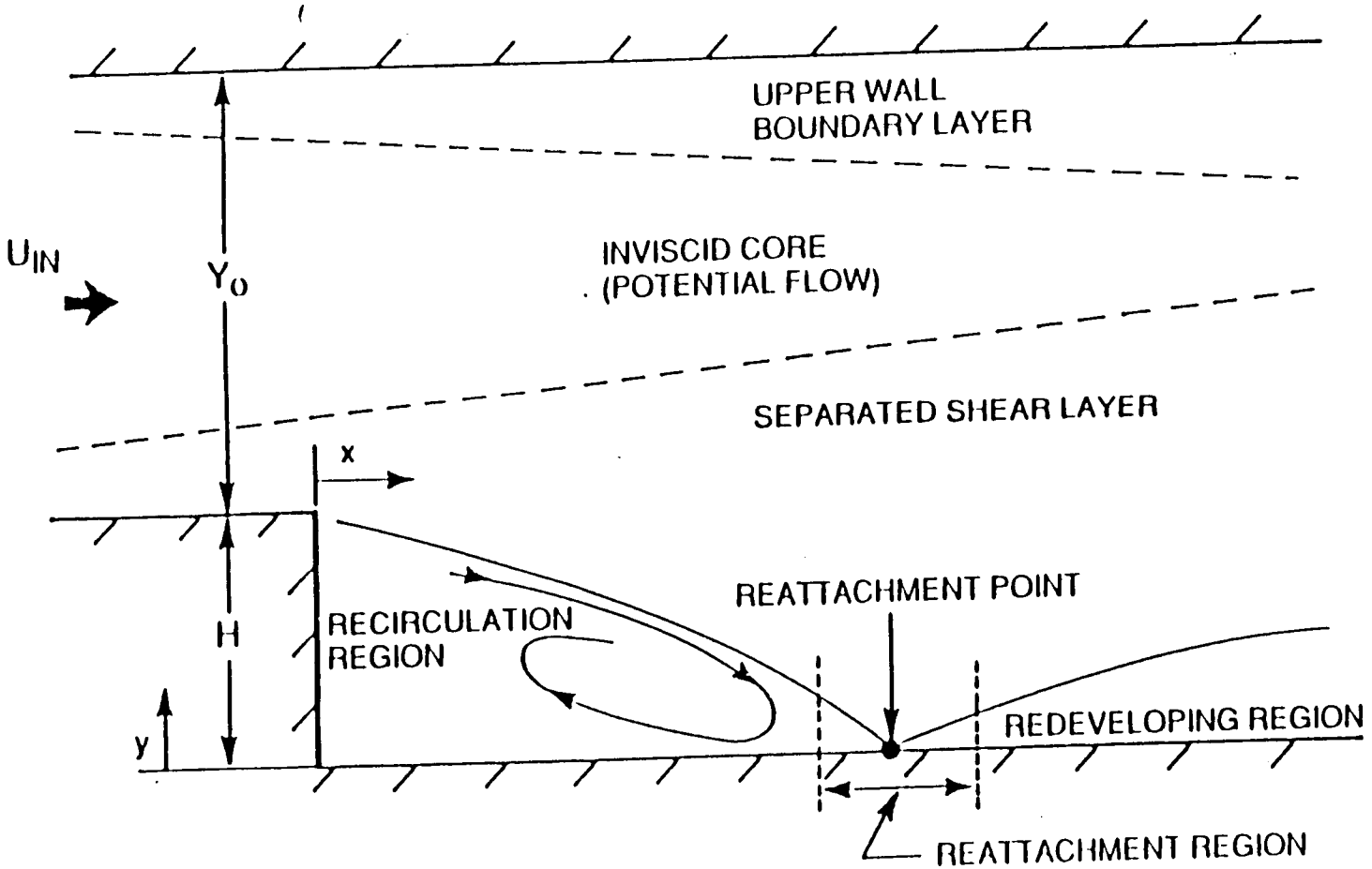

Figure 1 Solution domain -- Backward-facing geometry with the separating, recirculation and redeveloping regions.

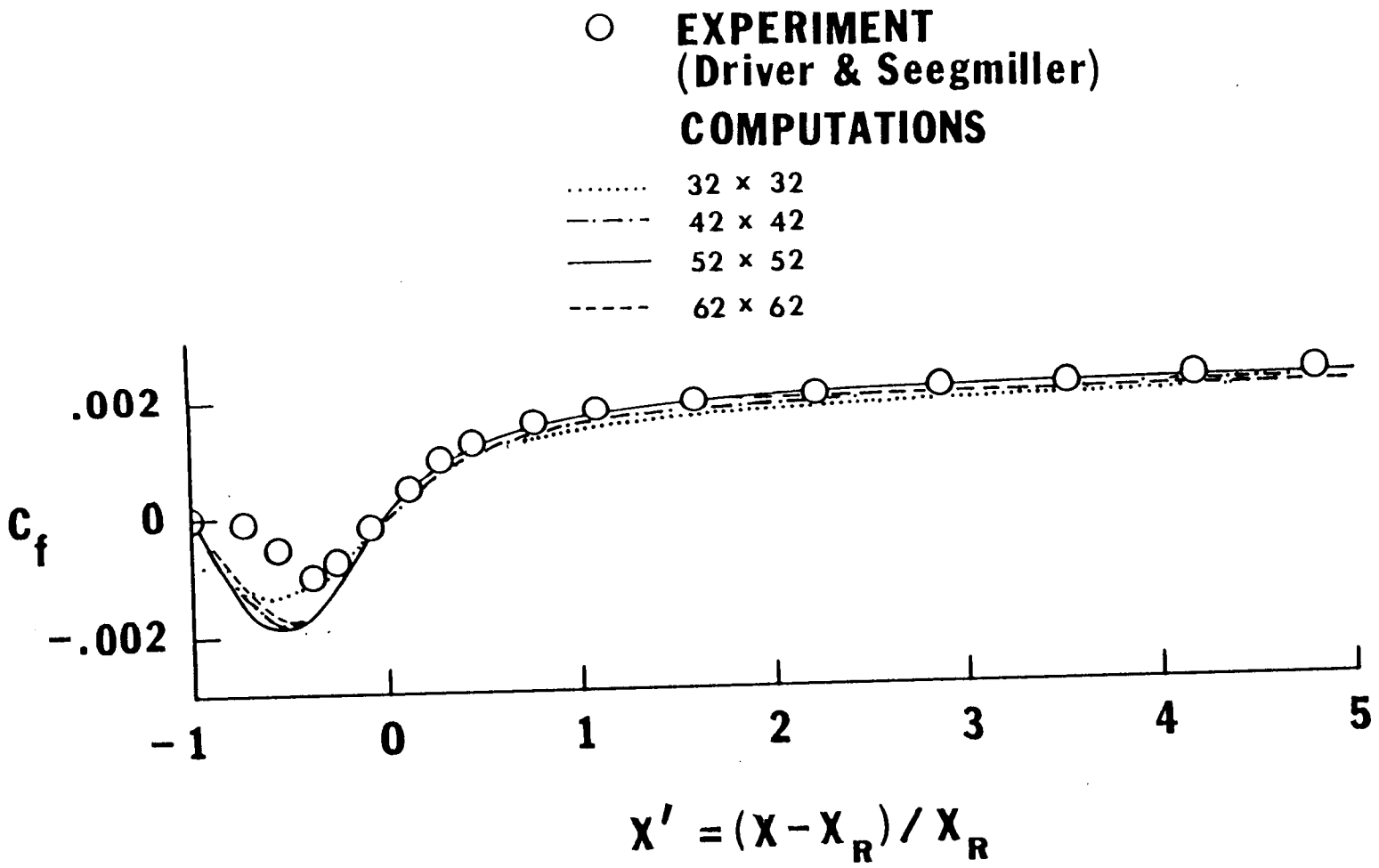

Figure 2 Skin friction coefficient along the bottom wall downstream on the step.

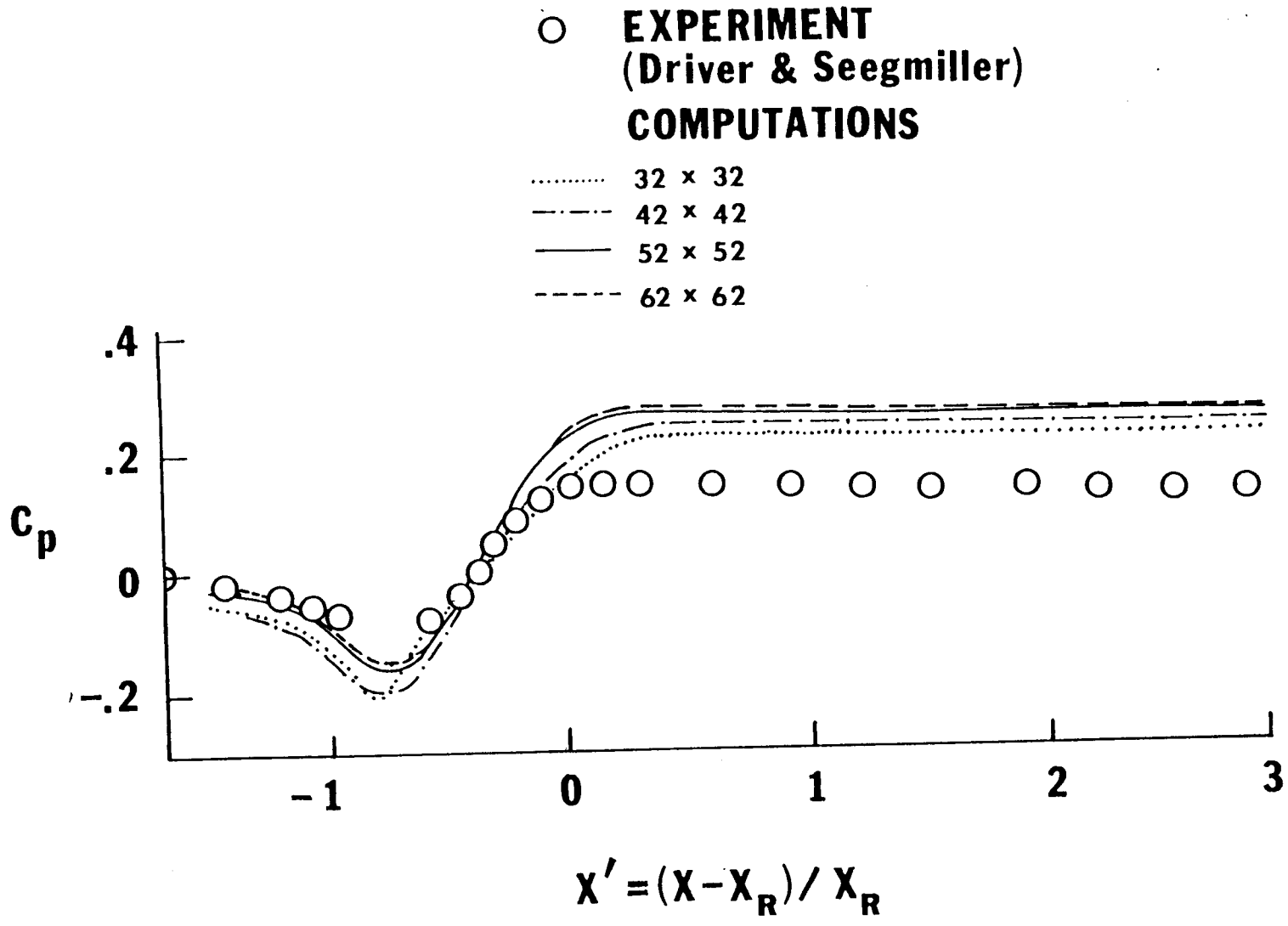

Figure 3 Pressure coefficient along the bottom wall downstream of the step.

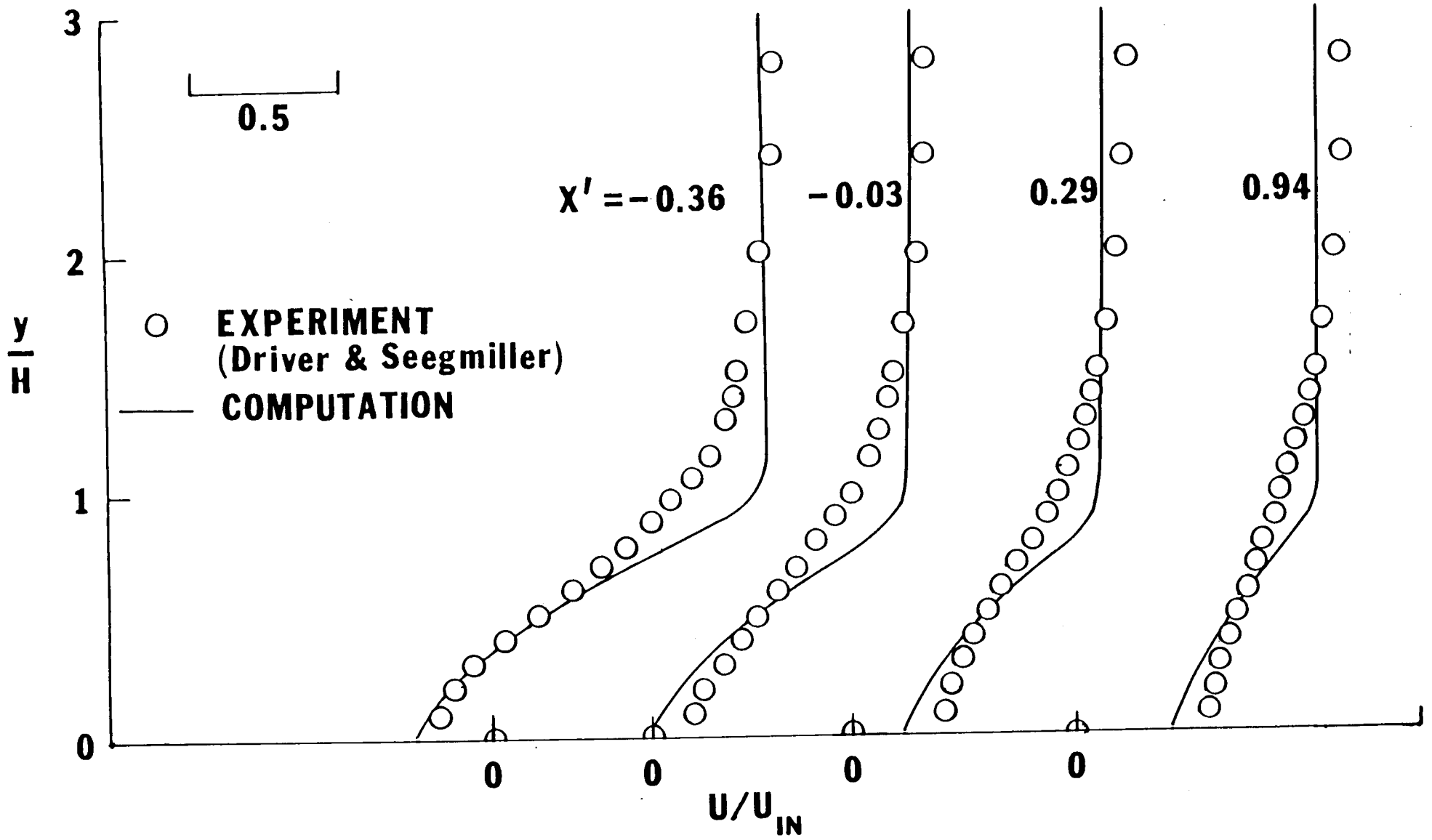

Figure 4 U-velocity profiles downstream of the step.

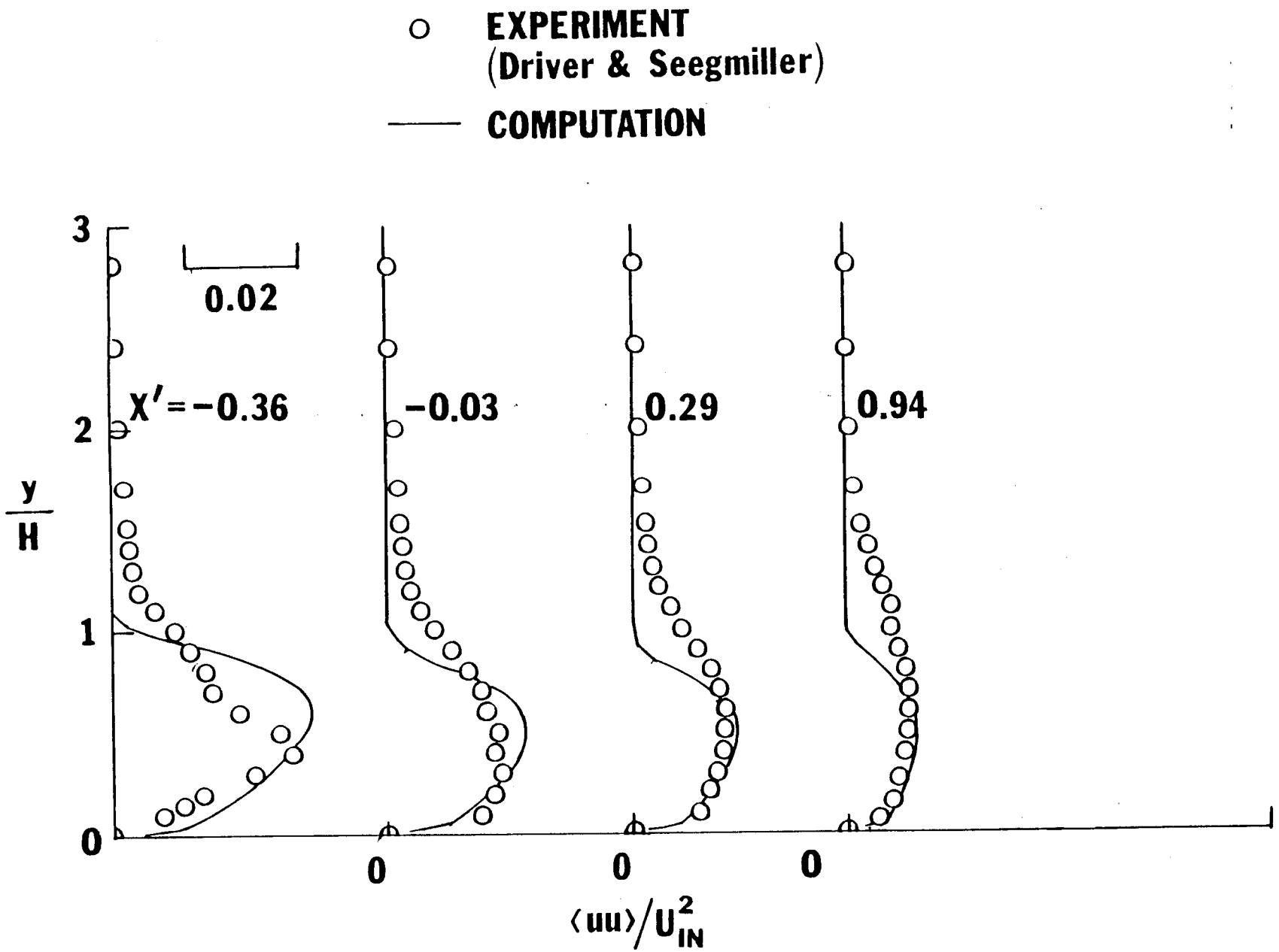

Figure 5 <uu>-profiles downstream of the step.

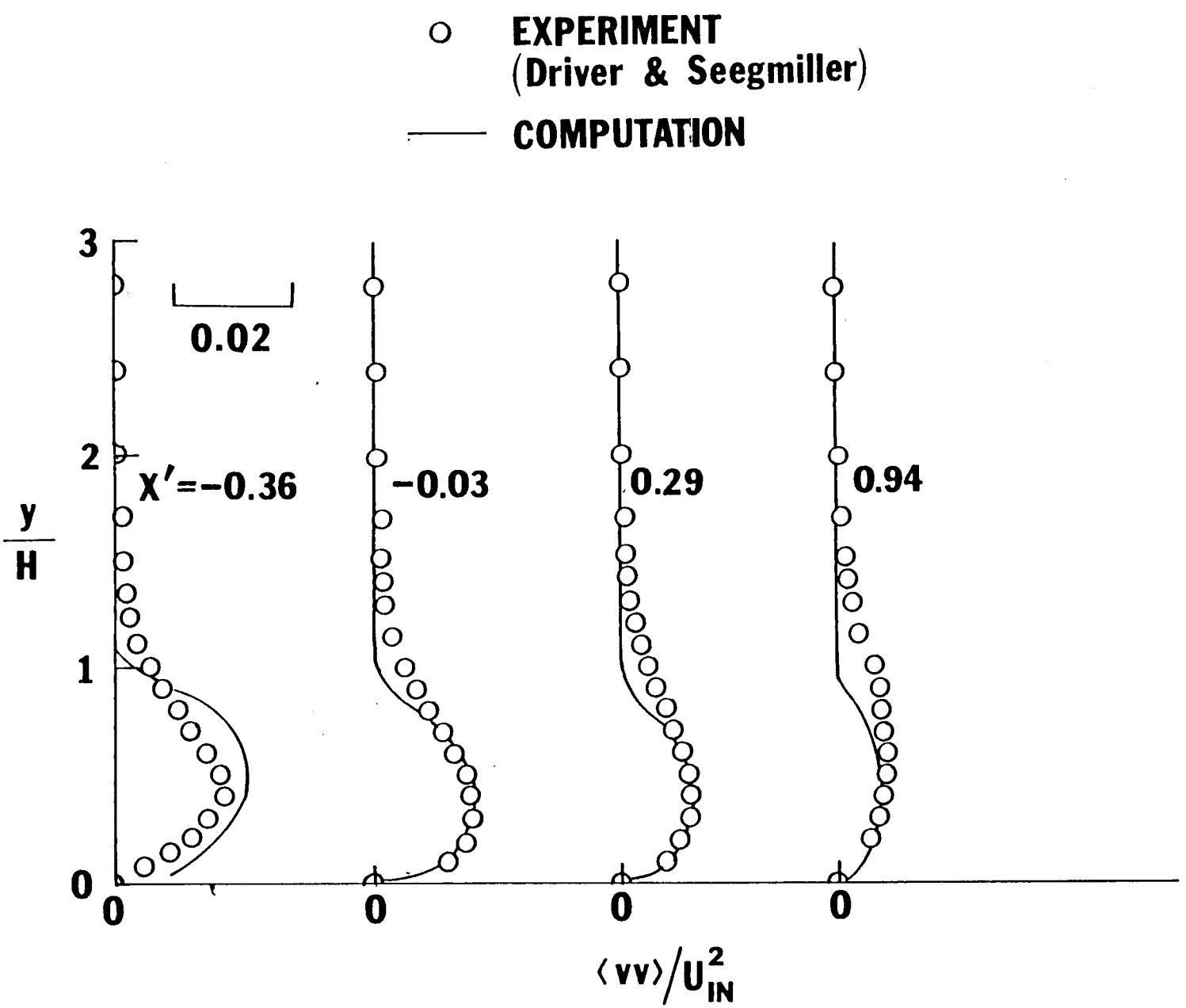

Figure 6 <vv>-profiles downstream of the step.

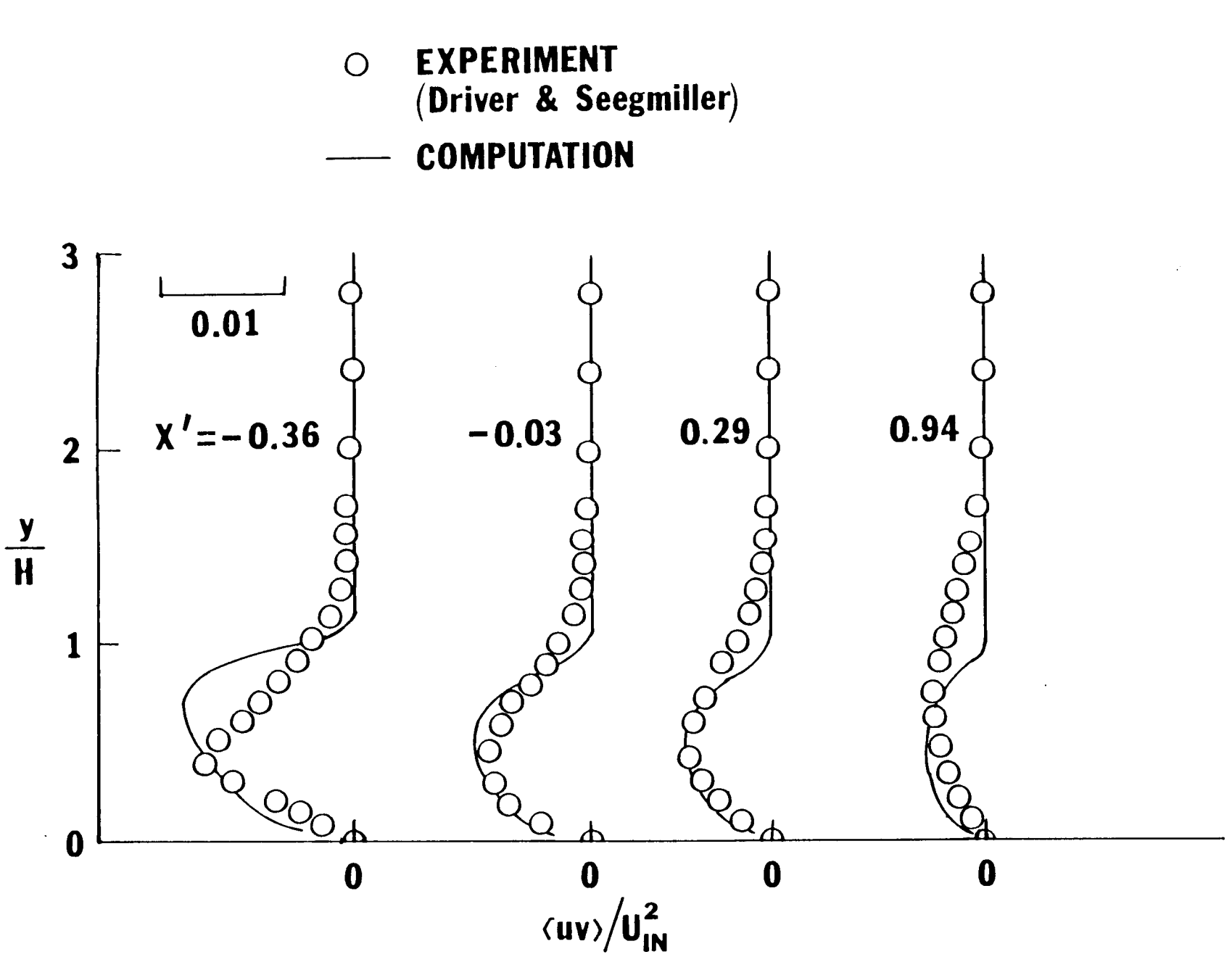

Figure 7 <uv>-profiles downstream of the step.

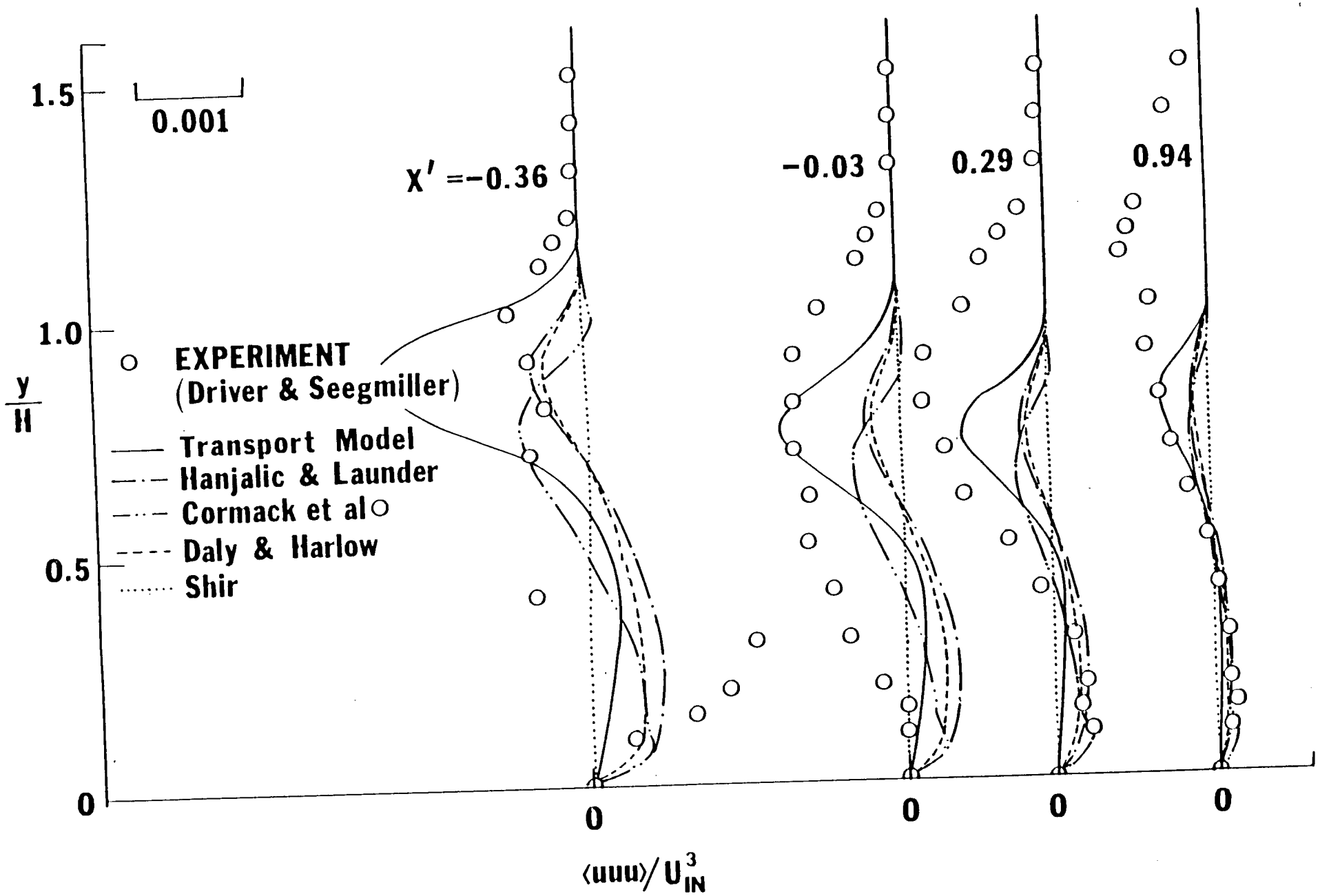

Figure 8 <uuu>-profiles downstream of the step.

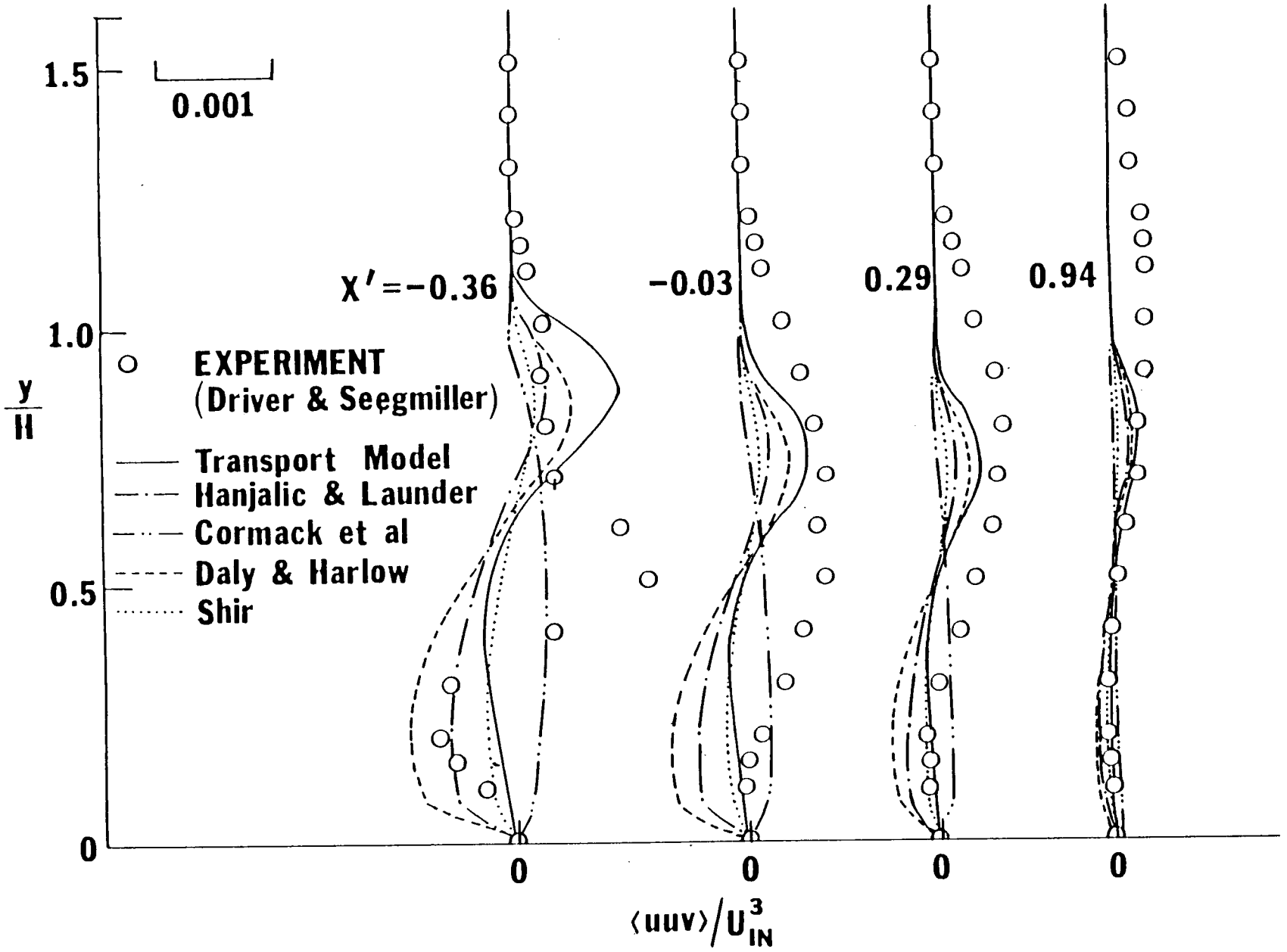

Figure 9 <uuv>-profiles downstream of the step.

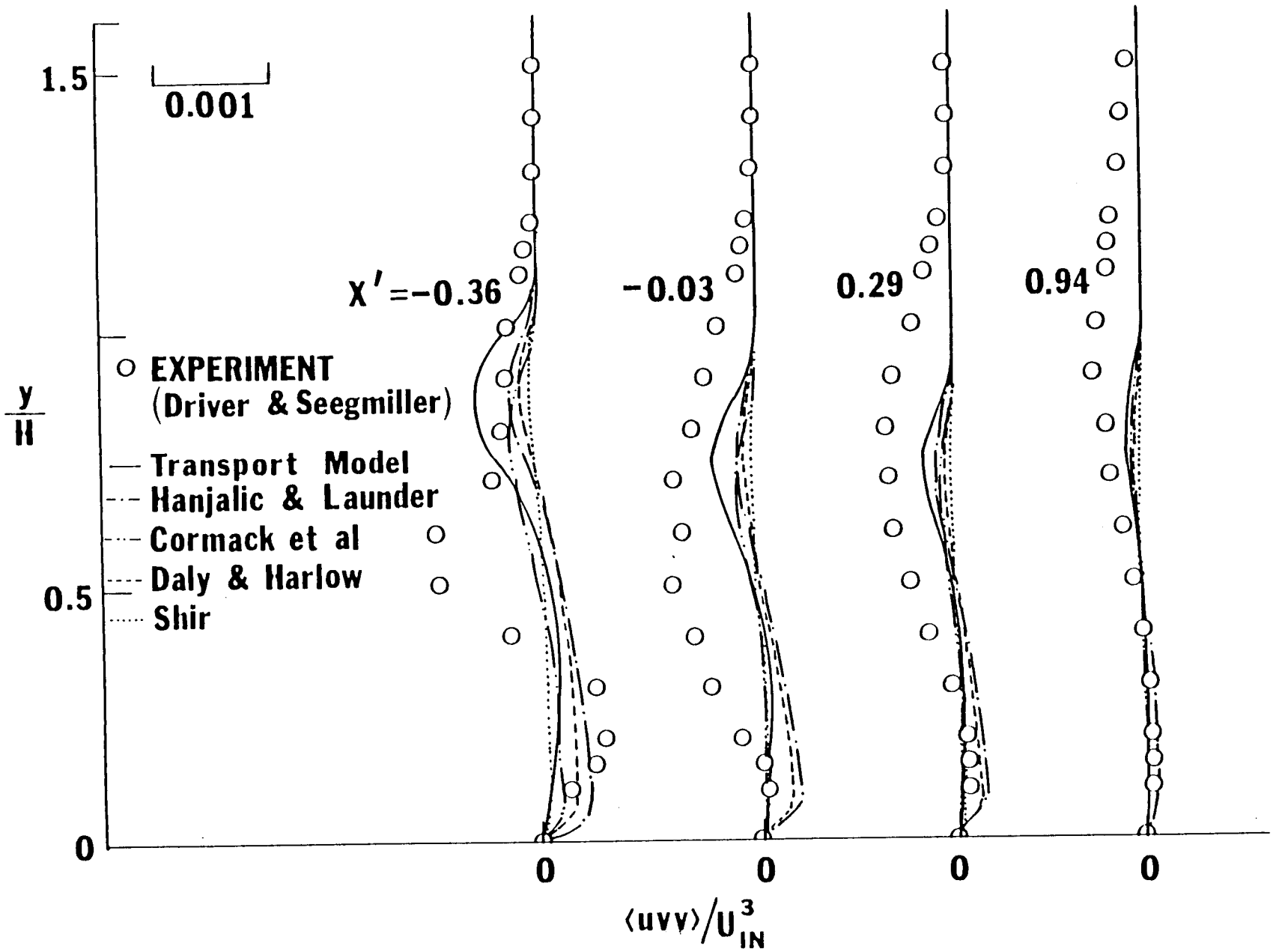

Figure 10 <uvv>-profiles downstream of the step.

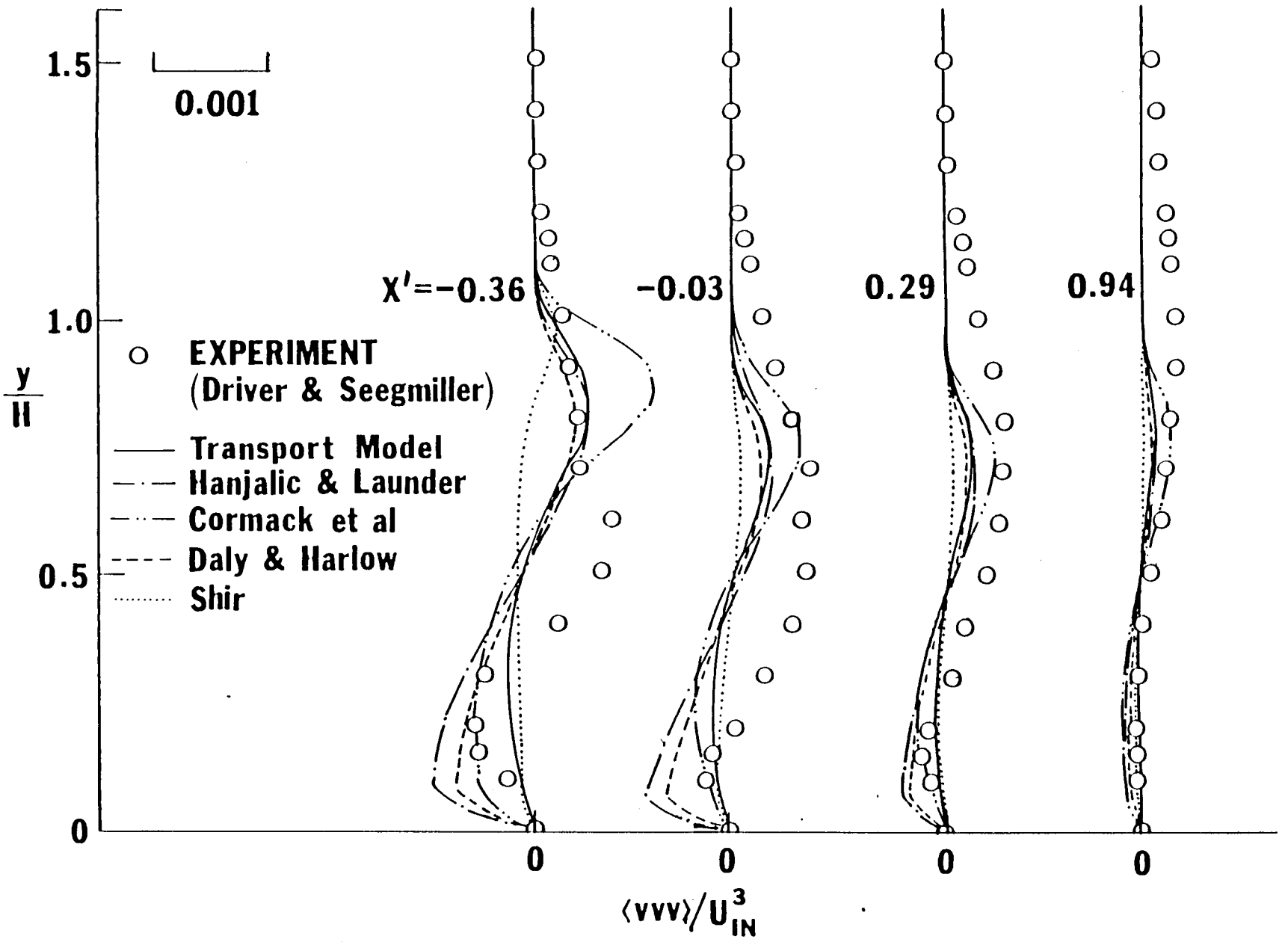

Figure 11 <vvv>-profiles downstream of the step.

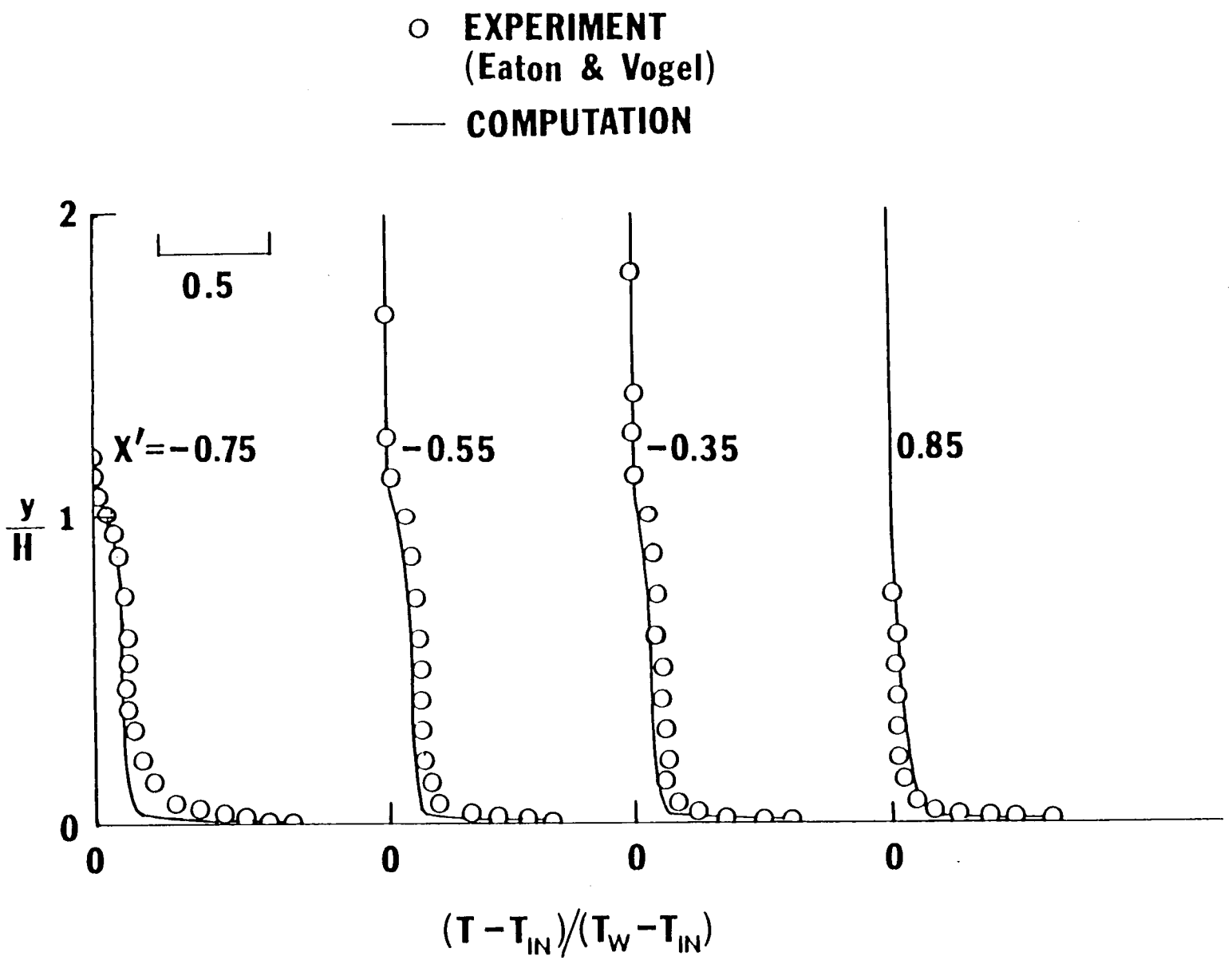

Figure 12 T-profiles downstream of the step.

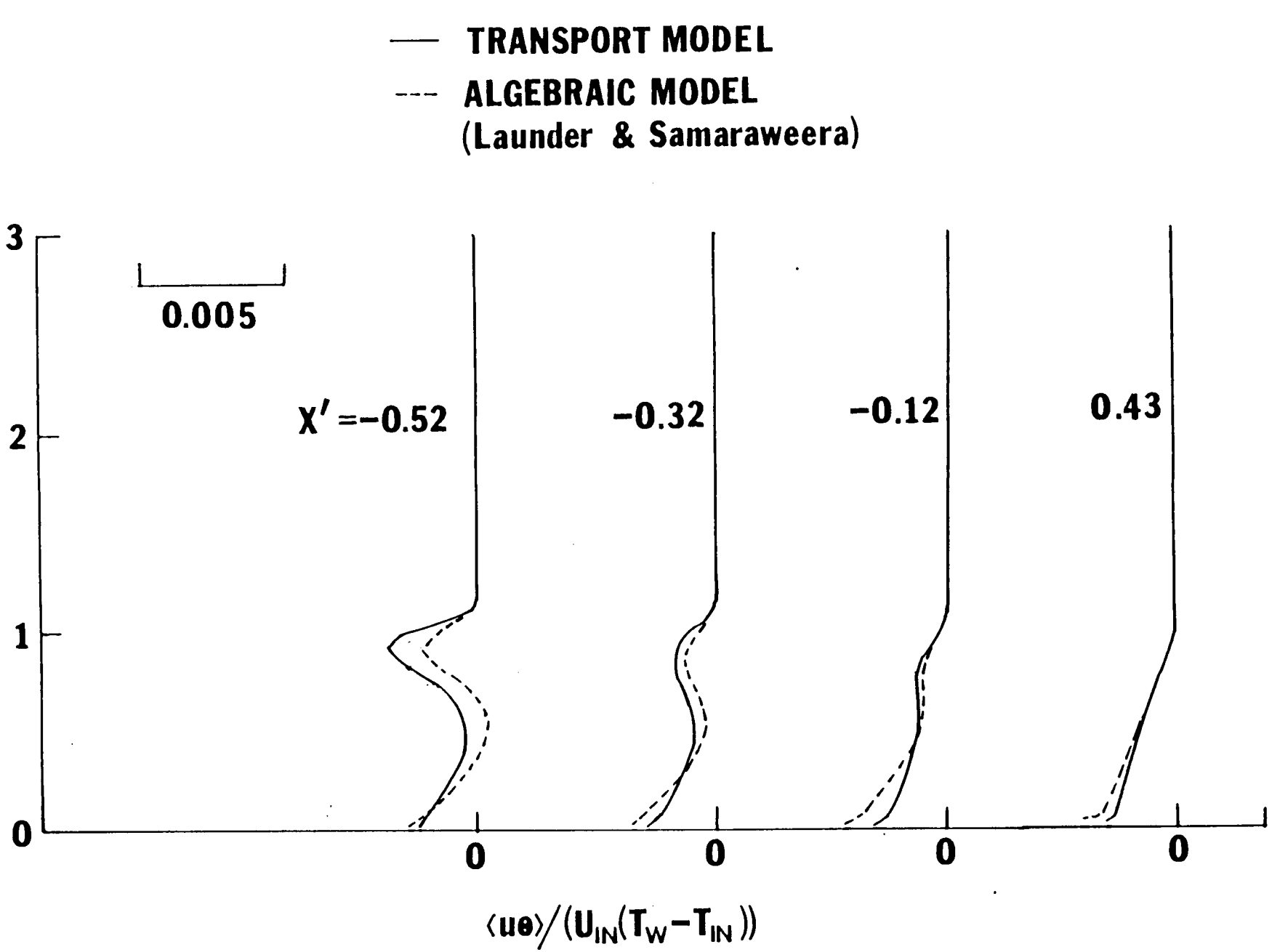

Figure 13 <uθ>-profiles downstream of the step.

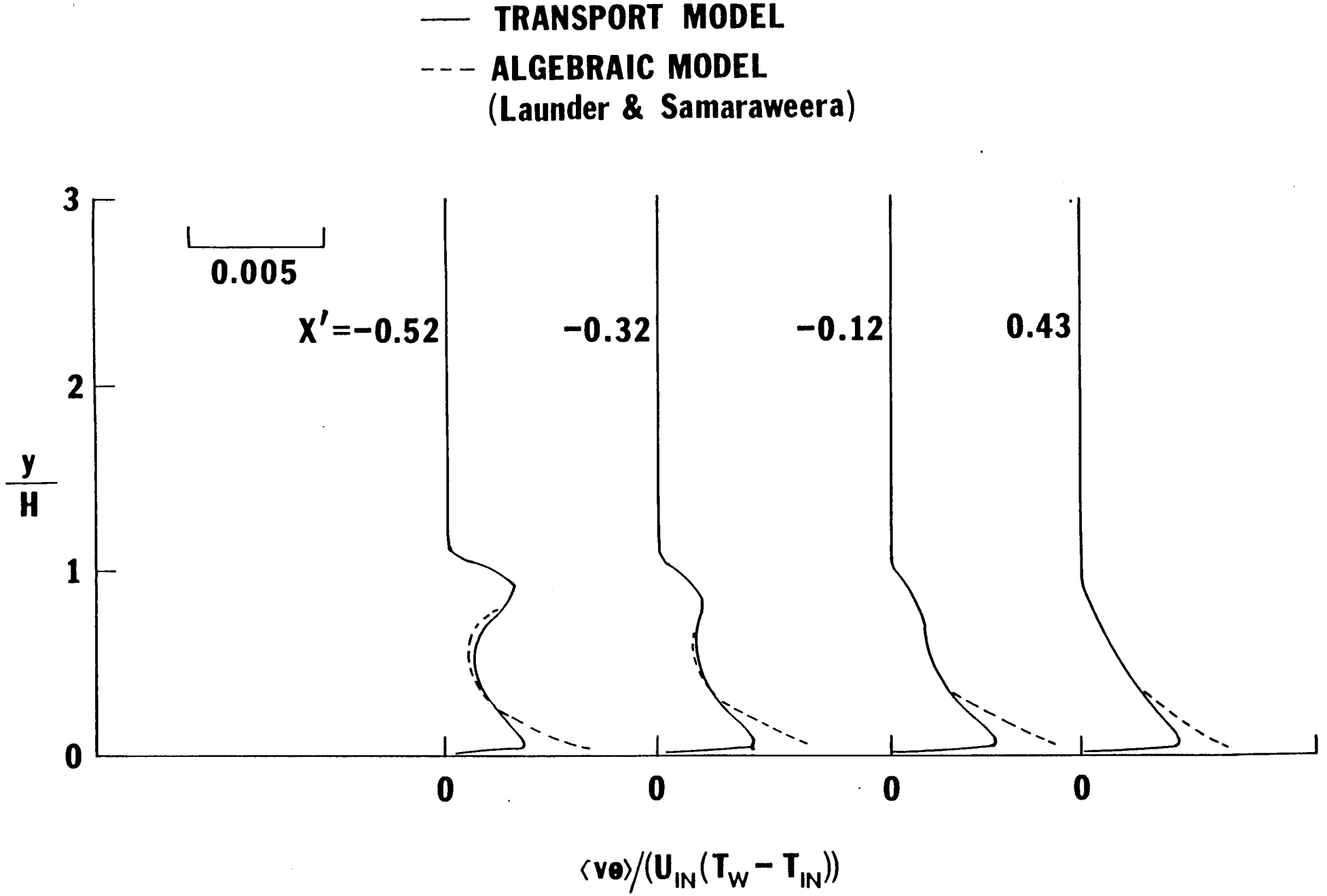

Figure 14 <vθ>-profiles downstream of the step.

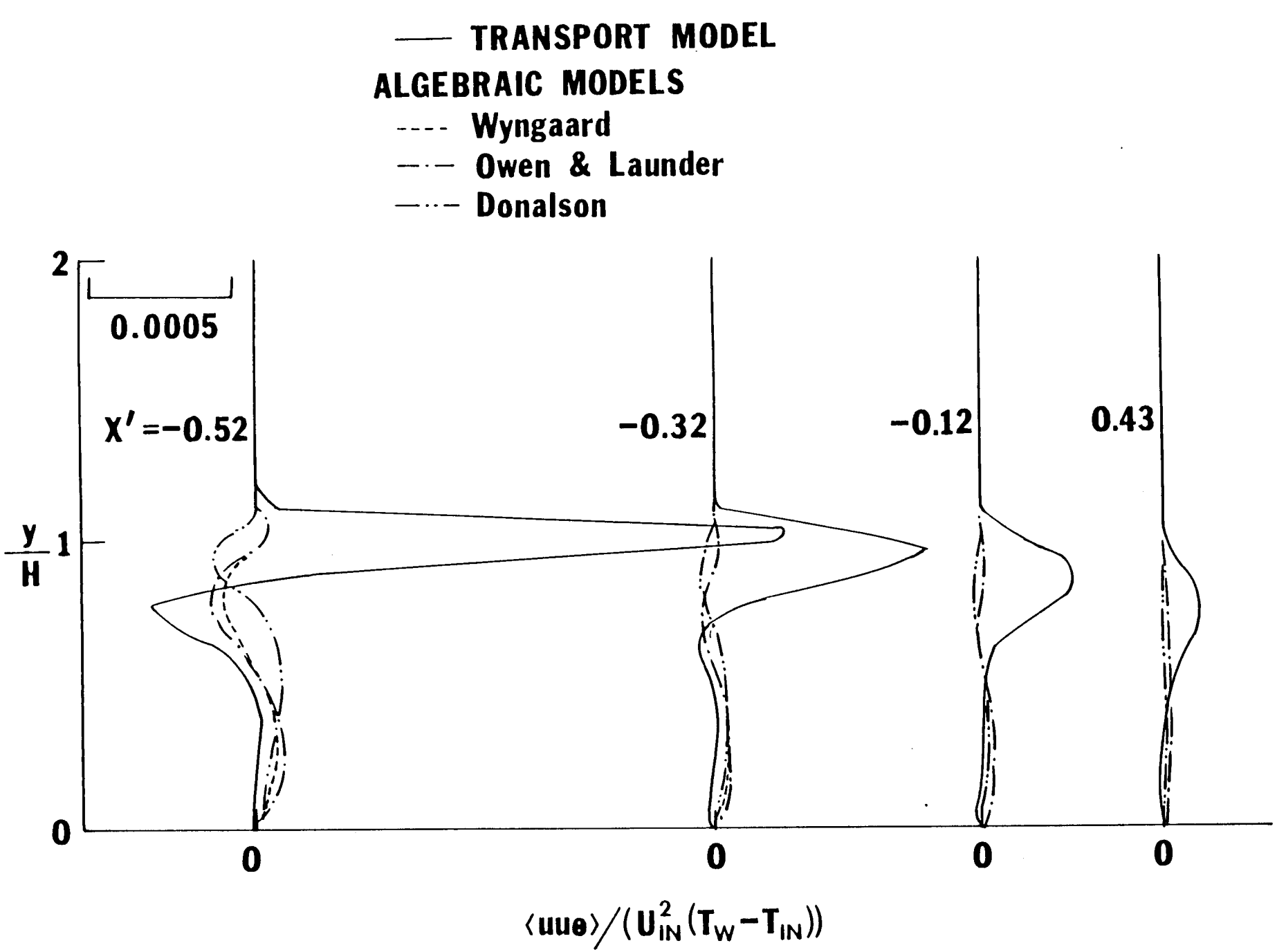

Figure 15 <uuθ>-profiles downstream of the step.

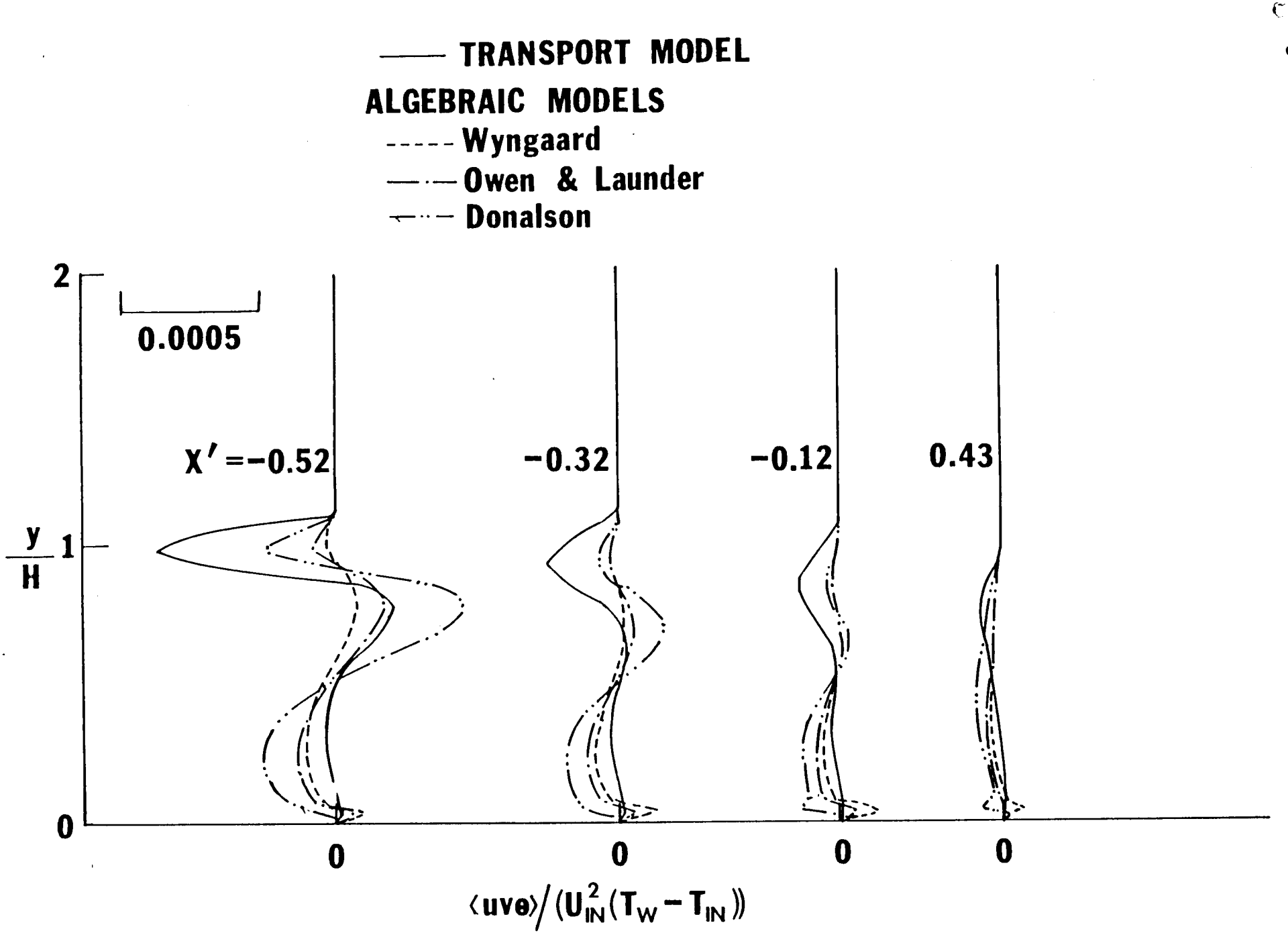

Figure 16 <uvθ>-profiles downstream of the step.

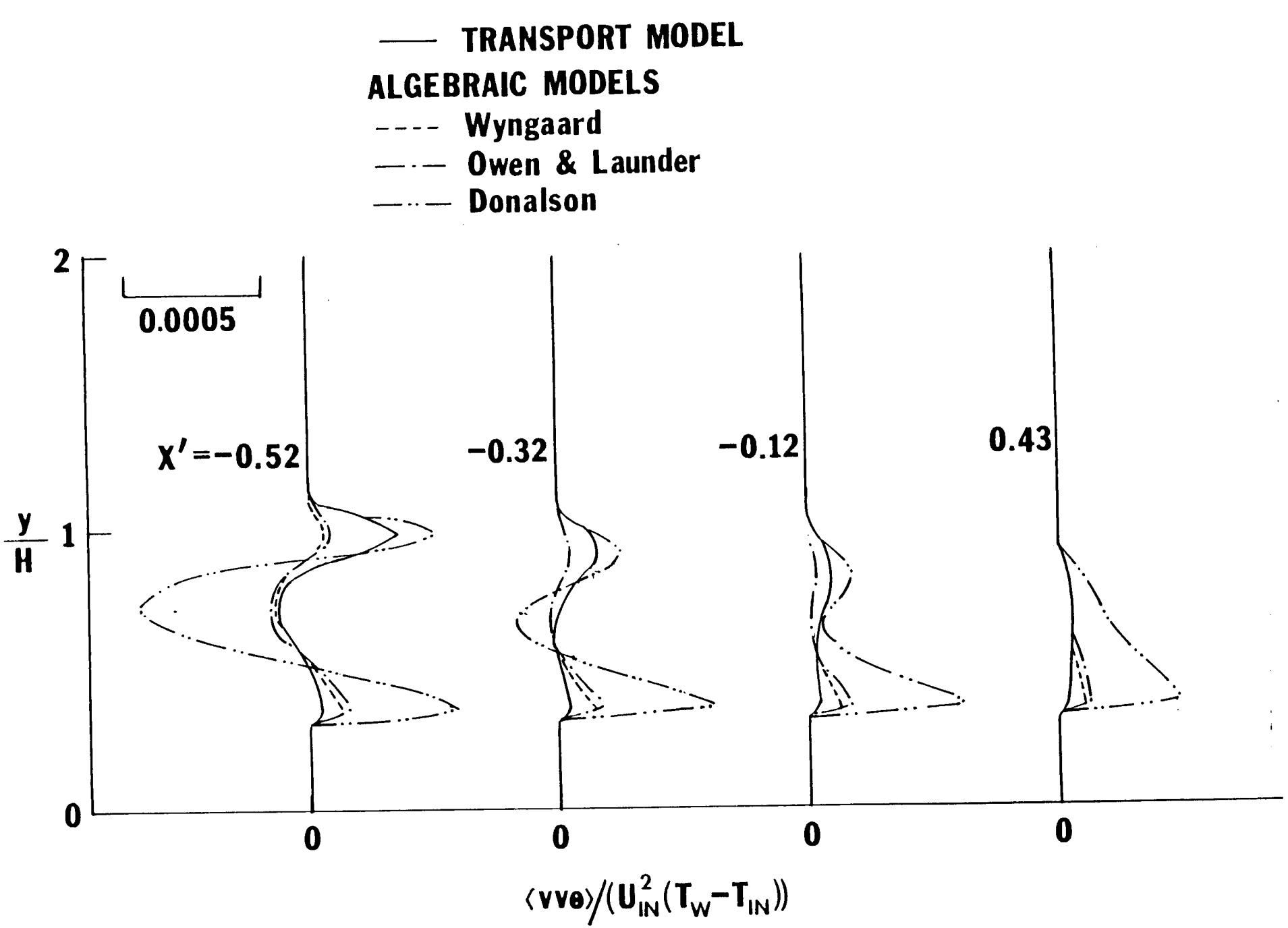

Figure 17 <vvθ>-profiles downstream of the step.